Earth Planets Space, **59**, 553–559, 2007

Seismic moment of the 1891 Nobi, Japan, earthquake estimated from historical seismograms

Eiichi Fukuyama[1], Ikuei Muramatu[2], and Takeshi Mikumo[3]

[1]*National Research Institute of Earth Sciences and Disaster Prevention, Tsukuba 305-0006, Japan*
[2]*Emeritus professor of Gifu University, Gifu 2435-62, Japan*
[3]*Instituto de Geofisica, Universidad Nacional Autonoma de Mexico, Mexico 04510 D.F., Mexico*

(Received September 6, 2006; Revised April 11, 2007; Accepted April 15, 2007; Online published June 27, 2007)

The seismic moment of the 1891 Nobi, Japan, earthquake has been evaluated from the historical seismogram recorded at the Central Meteorological Observatory in Tokyo. For this purpose, synthetic seismograms from point and finite source models with various fault parameters have been calculated by a discrete wave-number method, incorporating the instrumental response of the Gray-Milne-Ewing seismograph, and then compared with the original records. Our estimate of the seismic moment (M_o) is 1.8×10^{20} N m corresponding to a moment magnitude (M_w) 7.5. This is significantly smaller than the previous estimates from the distribution of damage, but is consistent with that inferred from geological field survey (Matsuda, 1974) of the surface faults.
Key words: Seismic moment, historical seismograms, the 1891 Nobi earthquake.

1. Introduction

The October 28, 1891 Nobi earthquake was the greatest inland earthquake ever experienced on the Japanese Islands. Its magnitude has been first estimated as 7.9 in Japan Meteorological Agency (JMA) scale (Japan Meteorological Agency, 1957), and later re-estimated as about 8.0 (Muramatu, 1962) from the distribution of seismic intensities around the epicentral region. The seismic moment of this large event, however, has not been evaluated so far directly from seismic observations at that time. It had been reported (Gifu Observatory, 1894) that the great earthquake was recorded at five stations: Gifu Weather Observatory, Nagoya Weather Observatory, Osaka Weather Observatory, Central Meteorological Observatory (CMO) in Tokyo, and the Imperial University of Tokyo, by the Gray-Milne-Ewing type (GME) seismographs. Although the seismograms recorded at the first two stations have been used to infer the overall features of faulting process of this earthquake (Mikumo and Ando, 1976), these records unfortunately went off scale at about 8.5 s at Gifu and at about 13.5 s at Nagoya after triggering. This saturation might be due to the arrival of large amplitude S-waves, and hence is not appropriate to estimate the total seismic moment.

We have been looking for old seismograms from the other three stations, as well as from then-existed worldwide stations, and we are now able to obtain the historical seismograms recorded at the CMO, by the courtesy of a personnel at the present Japan Meteorological Agency*. A direct estimate of seismic moment from these seismograms would provide some constraints on the entire faulting process of this unusually great earthquake. In this article, we are making various calculations by applying a recent computational technique to evaluate the seismic moment and its corresponding moment magnitude. The results could be discussed along with another study on dynamic rupture propagation during this earthquake (Fukuyama and Mikumo, 2006).

2. Data Processing

Figure 1 shows the original, two horizontal- and a vertical-component seismograms from the 1891 earthquake, which had been recorded by the GME instrument at the CMO station. The mechanical seismograph has a pendulum of 2 kg-weight, a natural period of 3 seconds, and a magnification of 5–5.5 for the horizontal component and about 9–10 for the vertical component, respectively (Gifu Observatory, 1894). In the present study, we assumed the amplification factor for horizontal components as 5. The damping factor is not well known, but estimated as about 0.1 due to friction between the pen-tip and a recording paper (Mikumo and Ando, 1976). Since the recorded trace of the original seismograms were overlapped several times as shown in Fig. 1, we first traced each waveform very carefully as shown in Fig. 2. Then the traced original seismograms are digitized and corrected for curved traces for large amplitudes by estimating the arm-length of the recording-pen and the recorded offsets on a trial- and error-technique. The corrected seismograms are shown in Fig. 3.

3. Calculations for Synthetic Seismograms

Now we calculate synthetic seismograms that would be observed at the CMO station in Tokyo, which is located at about 300 km east from the epicentral zone. The technique applied here is the discrete wave-number method by

*The original record is stored at Tokyo District Meteorological Observatory, Japan Meteorological Agency, and can be accessed upon request.

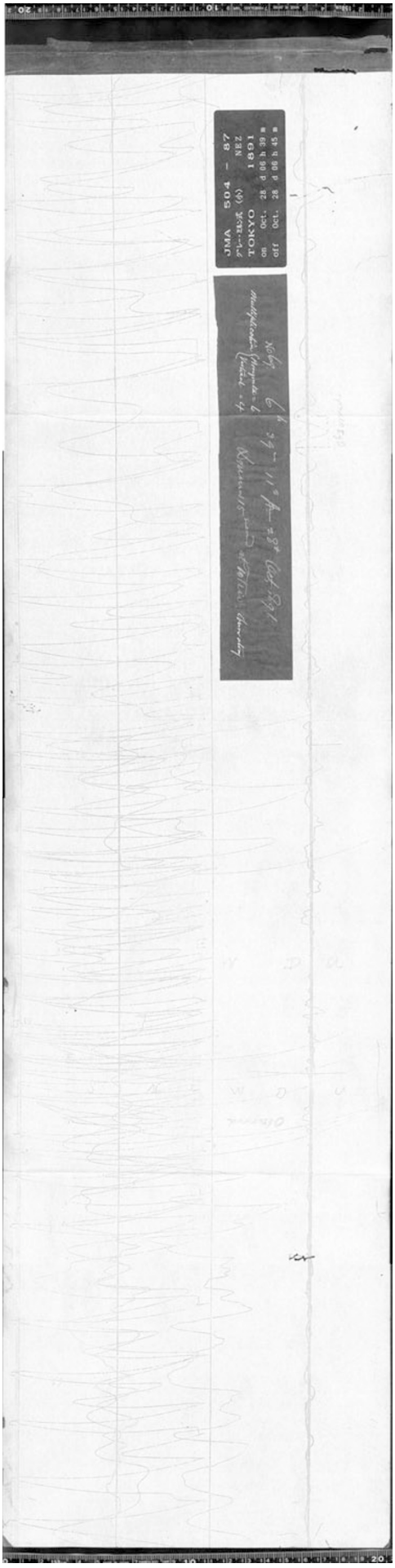

Fig. 1. Original seismograms recorded during the 1891 Nobi earthquake by the GME-type seismograph at the Central Meteorological Observatory in Tokyo. Black and white colors are exchanged to make it clearly visible.

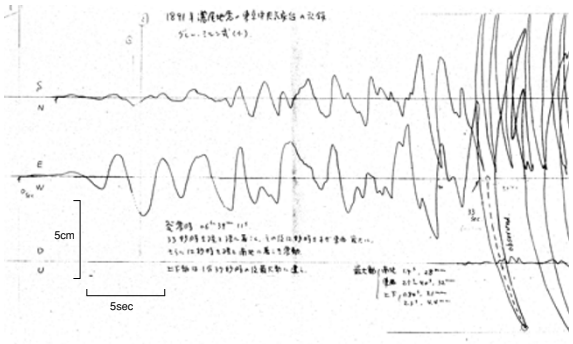

Fig. 2. Hand-traced seismograms used for the digitization process.

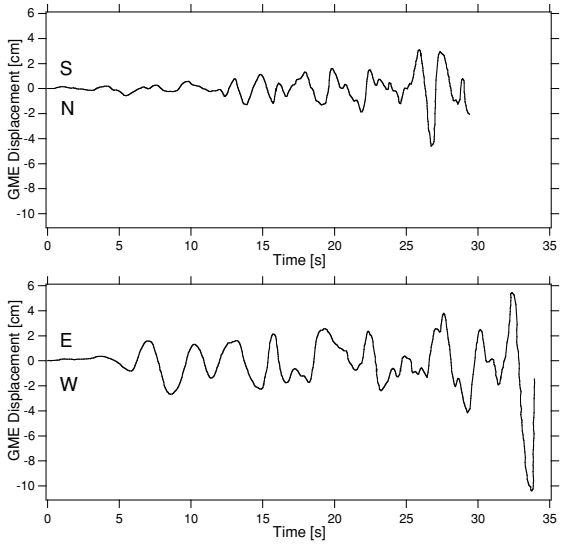

Fig. 3. The arm-length corrected two horizontal-component seismograms. The time starts at the trigger time of the seismogram.

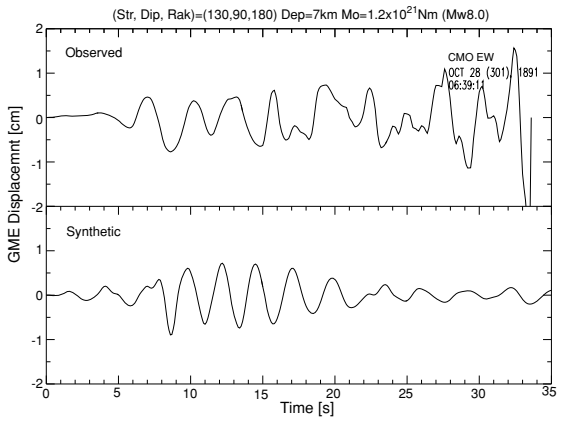

Fig. 4. A comparison between the EW-component record and the synthetic seismogram for a point-source model.

Saikia (1994) for a 1-D horizontally-layered crustal structure, which is routinely used for the determination of regional moment tensors in Japan (Fukuyama *et al.*, 1998; Kubo *et al.*, 2002). The instrumental response of the GME seismograph is then incorporated to compare the calculated synthetics with the observed seismograms.

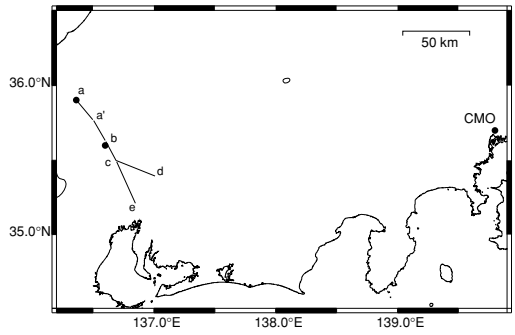

Fig. 5. Fault model (solid lines) and the location of CMO station (solid circle in the right hand side) are shown. Rupture initiation point (close to 'a') and point source location (close to 'b') are shown as solid circles in the left hand side.

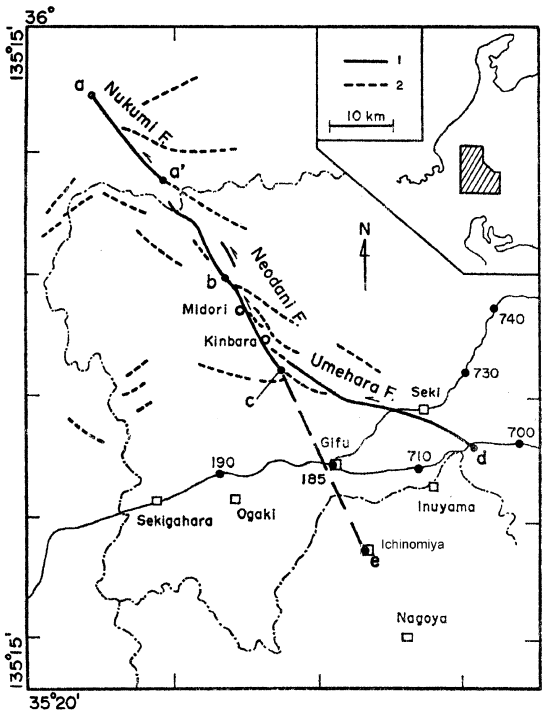

Fig. 6. Fault traces (thick solid lines) during the 1891 earthquake (Matsuda, 1974), and an assumed buried fault (dotted line) along the Gifu–Ichinomiya line (Mikumo and Ando, 1976).

3.1 A point-source model

Since the detailed rupture propagation history is not well known for this earthquake, we first tried to calculate the synthetics using a point source model by searching for various parameters including the dip and strike angles in the faulting mechanism, focal depth, seismic moment, and instrumental constants. It is found that the assumed seismic moment is a most sensitive parameter in comparing the calculated synthetics with the waveform and amplitude of the original records.

Figure 4 shows its comparison between the EW-component record and the synthetics for a tentative seismic moment of $M_o = 1.2 \times 10^{21}$ N m ($M_w = 8$), with a focal depth of 7 km and a mechanism with (strike, dip, rake) = (N130°E, 90°, 100°). In this case, the location of the point source is tentatively taken at the center of the Neodani fault

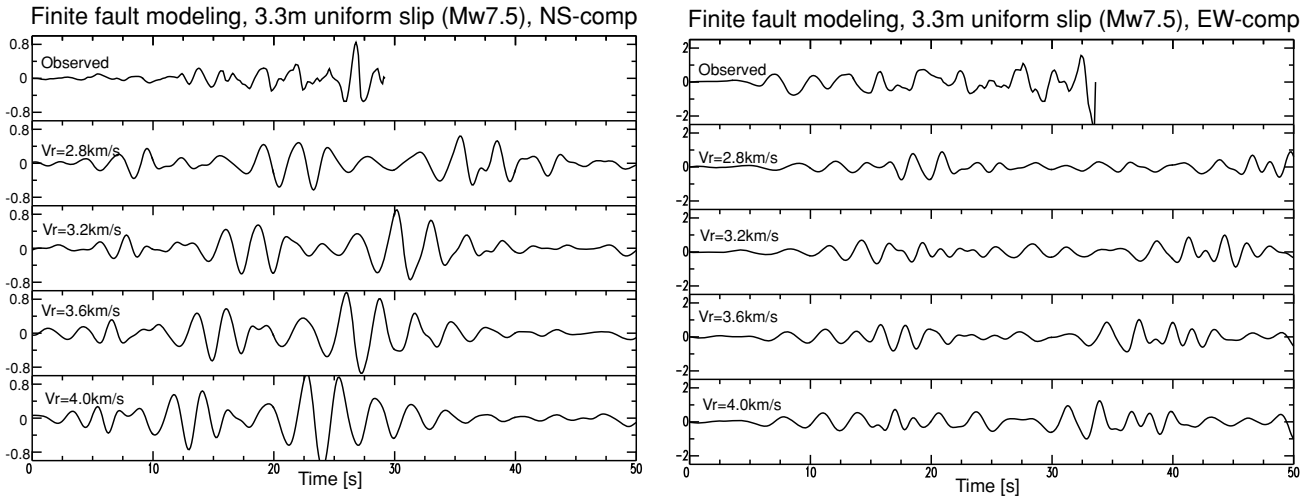

Fig. 7. Comparison between the two horizontal-component records and the synthetic seismograms from a finite source model for different rupture velocities with an assumed uniform slip of 3.3 m.

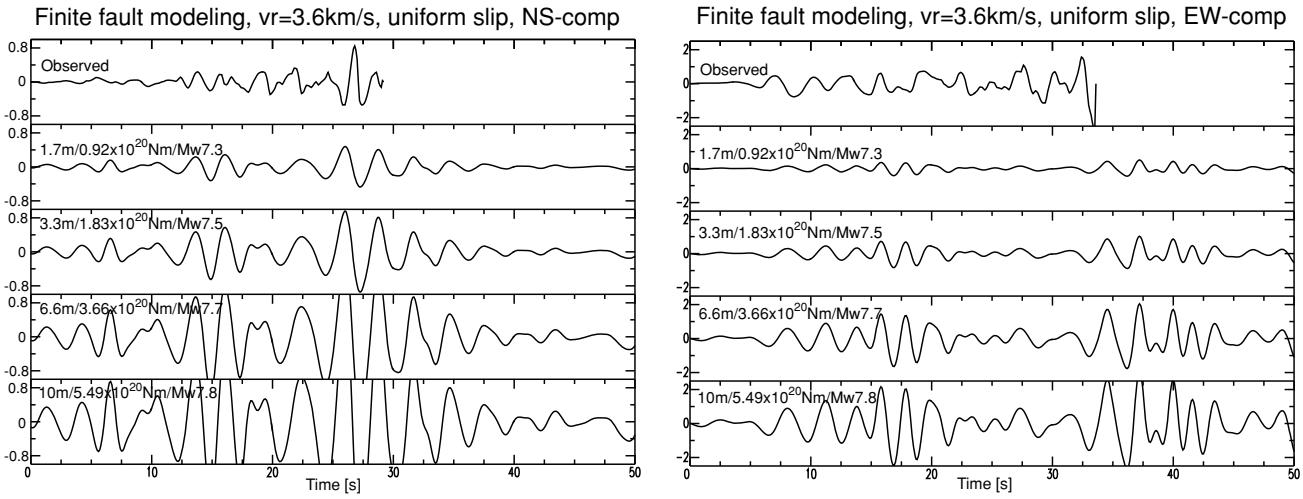

Fig. 8. Comparison between the two horizontal-component records and the synthetic seismograms from a finite source model for different seismic moment with a fixed rupture velocity of 3.6 km/s.

(Matsuda, 1974) as shown in Fig. 5.

Because the epicentral distance between the assumed source and the CMO station is about 300 km, which is not far enough as compared with the actual fault dimension of this earthquake (∼80 km), we believe it is essential to include a finite fault dimension into the calculation of the synthetic seismograms.

3.2 Geometry of the faults

The surface fault breaks appeared over 80 km long during this great earthquake, which have been traced initially by Koto (1893) and Omori (1900), and later by Matsuda (1974) from detailed field surveys. Figure 6 shows these main fault traces based on Matsuda's survey, and Table 1 summarizes their length, strike, dip, rake and depth range (Fukuyama and Mikumo, 2006; modified from Mikumo and Ando, 1976). The surface fault consists of three major segments: Nukumi (a–a′), Neodani (a′–b–c), and Umehara (c–d) faults. In addition, a possible existence of a buried vertical fault (c–e), which is called the Gifu–Ichinomiya line, has been suggested from various data (e.g. Muramatu, 1963; Mikumo and Ando, 1976; Sugisaki and Shibata, 2003). Recent numerical simulations of dynamic rupture propagation (Fukuyama and Mikumo, 2006) also suggest the existence of the buried fault.

3.3 Finite source models

3.3.1 Contribution from each fault segment In Fig. 5 and Table 1, the fault model for the computation of synthetic seismograms is shown, which is based on the model of Mikumo and Ando (1976). The bottom depth of all the fault segments is assumed to be 15 km from micro-earthquake distribution around this area (Ooida *et al.*, 1971). We assume that the fault rupture initiated from the northwestern end (a in Fig. 5) of the Nukumi fault at a depth of 10 km and propagated radially with a constant velocity to the other faults. We do not consider the rupture time gap between the fault segments. The rupture starting point has been inferred from S-P times and a comparison between the recorded and calculated waveforms at the Gifu and Nagoya stations, and also from the predominant directions of strong ground motion at various sites (Mikumo and

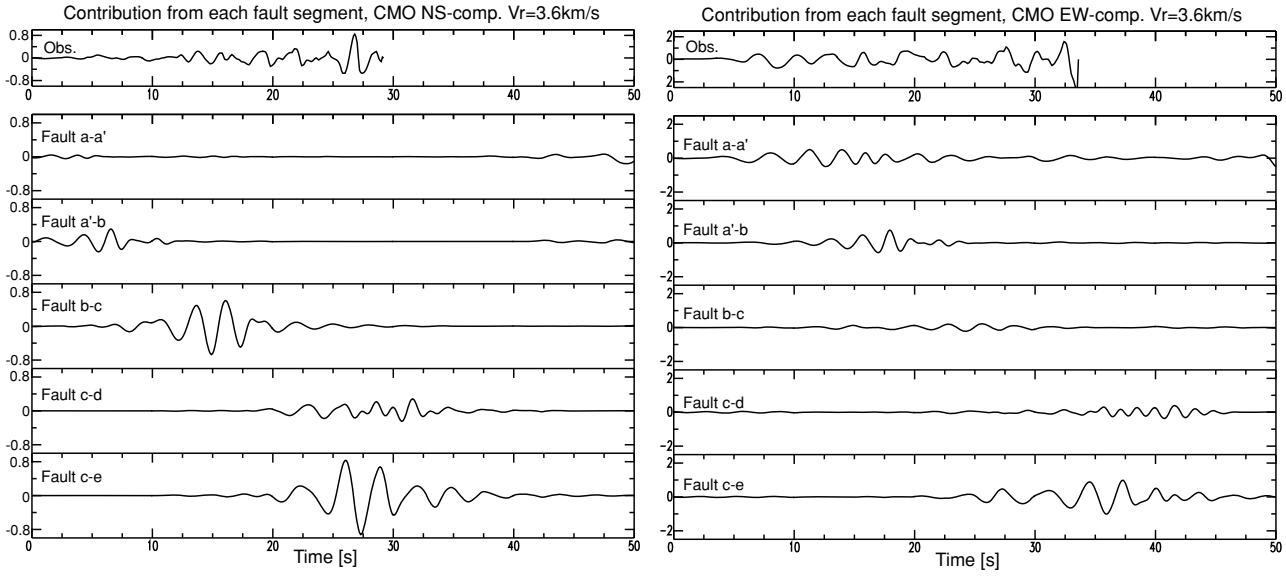

Fig. 9. The synthetic seismograms from each fault segment of a finite source model.

Ando, 1976).

Here we calculate the synthetic seismograms for two horizontal components at CMO based on the finite source model, taking into account the above information on the surface fault breaks and the buried fault. In the following computation, we tried to find suitable parameters of rupture velocity and seismic moment by a trial and error method in a forward modeling. We did not introduce an error function to evaluate the fit of synthetic waveforms but we judged by eyes to observe the fit of wave-train arrivals. This is because the error function is usually affected by the detailed phase difference, which we did not focus on in this analysis. In addition, since only one station was available for the estimation of these parameters, we assume that a constant rupture velocity and a uniform final slip on the fault and they are the same on all fault segments. We used a rise time of 2 seconds, which was insensitive to the synthetic seismogram because rather long period waveforms are dominated in the observed seismogram.

3.3.2 Effects of rupture velocity Figure 7 shows the synthetic waveforms calculated for four different rupture velocities (V_r) ranging from 2.8 to 4.0 km/s with an assumed uniform slip of 3.3 m all over the fault segments (M_w 7.5). The calculated synthetics for the case of V_r = 3.6 km/s generates rather large-amplitude wave-train between 25 and 35 seconds, which appears generally consistent with the observed records given in the uppermost trace.

This rupture velocity estimated here is rather fast, but this velocity is consistent with Fukuyama and Mikumo (2006)'s dynamic rupture simulation, where the rupture velocity becomes super-shear in order for the rupture to propagate along both branched fault segments. Mikumo and Ando (1976) estimated the rupture velocity of about 2.5 km/s, but they used the seismograms at Gifu and Nagoya in which only the initial part of the rupture (∼first 10 seconds) was recorded. Thus, the present estimate does not contradict to theirs.

3.3.3 Seismic moment In Fig. 8 are shown the synthetic seismograms for four different uniform slips ranging from 1.7 m to 10 m corresponding to seismic moment from 0.92 to 5.49 $\times$ 10^{20} N m (M_w = 7.3 – 7.8) for a fixed rupture velocity of 3.6 km/s. We see that the second trace for M_o = 1.83 $\times$ 10^{20} N m (M_w = 7.5) appears to approximately match the amplitude of the recorded seismogram (particularly of the NS-component) given in the uppermost trace.

Recently, Nakano *et al.* (2007) re-analyzed the fault model of this earthquake to explain the leveling survey data across the fault. They estimated the seismic moment M_o = 1.38 $\times$ 10^{20} N m (M_w = 7.4), which is consistent with our result.

Figure 9 shows the contribution from each of the five fault segments to the synthetic seismogram, i.e. each seismogram is computed for the case when only the corresponding fault ruptures. From this figure we can see how the observed seismograms are composed, by looking at the different arrival times of wave train.

The amplitude of each synthetic trace, except from segment c–d, appears to be proportional to the length of the segments (Table 1), because we simply assume a uniform slip of 3.3 m on all the segments with a constant rupture velocity of 3.6 km/s. The difference between a′–b and b–c segments comes from the different fault rake (Table 1). Larger amplitude from segment c–e comes from its larger length of 35 km, while somewhat smaller amplitude from segment c–d may be due to its different strike with respect to the wave path to Tokyo. It should be noted that the slip directions shown in Table 1 are assumed to be consistent with the result of Mikumo and Ando (1976).

3.3.4 Possibility of rupture propagation on a buried fault along the Gifu–Ichinomiya line As have been discussed in the previous works (e.g. Muramatu, 1963; Mikumo and Ando, 1976; Fukuyama and Mikumo, 2006; Nakano *et al.*, 2007), it is probable that the rupture starting from the northwestern end (a) of the Nukumi fault branched

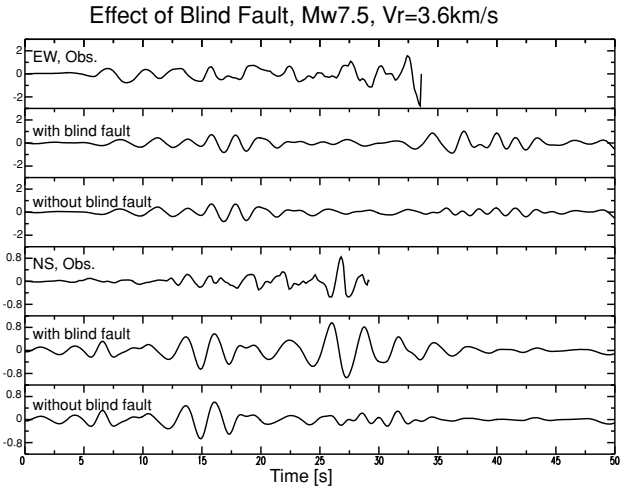

Fig. 10. Comparison between the two horizontal-component records and the synthetic seismograms from a finite source model with and without a buried blind fault (c–e).

off at point (c) and propagated along the Umehara fault (c–d) and also along the buried fault (c–e). To examine further this possibility, we calculate the synthetic seismograms for two different cases with and without this buried fault segment.

From the comparison between the synthetics and observed records, as shown in Fig. 10, it might be concluded that the rupture propagating towards the Gifu–Ichinomiya line (c–e) appears to favor the observed records, because of the arrival of large amplitude waves emitted from the c–e segment in the synthetic seismogram (Fig. 9) which is recognized in the observed waveforms. However, since we use the seismograms at only one station, we have to be careful in that the way of fitting to the observation might not be unique.

4. Discussions

The magnitude estimated here seems to be significantly smaller than the previously estimated magnitudes from the JMA scale (Japan Meteorological Agency, 1957) and also from the distribution of seismic intensities (Muramatu, 1962). This is not unreasonable, however, because the method of estimating the magnitude is entirely different. The previous estimates mainly depend on the distribution of damage, which might be amplified by the existence of the Nobi basin.

It is to be noted that the seismic moment estimated here is consistent with that inferred from a fault model (Mikumo and Ando, 1976) based on Matsuda's field survey (1974). Nakano *et al*. (2007) also obtained a similar seismic moment from the geodetic observations. In addition, the magnitude estimated here is consistent with the empirical relation proposed by Iida (1959) between magnitude and fault length.

It should also be noted that we used rather high frequency waves (∼3 s) to estimate the magnitude. Ideally, longer period seismic waves should be used for this purpose, which is independent of the detailed rupture process to measure the seismic moment. In the present case, however, since such long period information was not available, we assumed the rupture scenario to constrain the detailed rupture process. Then, seismic moment has been estimated from high frequency radiation. Although there are, of course, several possible scenarios for this earthquake, we assumed a simplest scenario that rupture propagates unilaterally with a constant rupture velocity and a uniform slip distribution. If more waveforms with broader frequencies were available at other stations, we would be able to place more constraints to the seismic moment.

5. Conclusions

We tried to evaluate the seismic moment of the 1891 great Nobi, Japan, earthquake from the historical seismogram recorded at the Central Meteorological Observatory (CMO) in Tokyo, which has been recently made available to us. To do this, we have calculated synthetic seismograms from point source and finite source models for a variety of fault parameters, by applying the discrete wave-number method for a horizontally-layered crustal structure. For the finite source models, we referred to the geometry of the four major fault segments revealed from Matsuda's field survey (1974), incorporating the possible existence of a buried fault along the Gifu–Ichinomiya line. From comparison between the observed two horizontal component records and the synthetic seismograms for a constant rupture velocity of about 3.6 km/s and a uniform slip of 3.3 m, we estimated the seismic moment of this earthquake as $M_o = 1.8 \times 10^{20}$ N m corresponding to a moment magnitude of $M_w = 7.5$. A comparison between the synthetics and the observed records appears to favor the existence of a buried fault along the Gifu–Ichinomiya line, although this inference is not conclusive because of a single station used here.

Acknowledgments. We are grateful to the staffs at Japan Meteorological Agency who provided the original seismograms recorded at CMO. We also appreciate the colleagues at UNAM who searched for other old seismograms at worldwide stations. Comments by Masaru Nakano, Sadaomi Suzuki and Naoshi Hirata were very helpful.

References

Fukuyama, E., M. Ishida, D. S. Dreger, and H. Kawai, Automated seismic moment tensor determination by using on-line broadband seismic waveforms, *Zisin (J. Seismol. Soc. Jpn.)*, Ser.2, **51**, 149–156, 1998 (in Japanese with English abstract).

Fukuyama, E. and T. Mikumo, Dynamic rupture propagation during the 1891 Nobi, central Japan, earthquake: Possible extension to branched faults, *Bull. Seism Soc. Am.*, **96**, 1257–1266, 2006.

Gifu Observatory, Report on the great Nobi earthquake, 1894 (in Japanese).

Iida, K., Earthquake energy and earthquake fault, *J. Earth Sci., Nagoya Univ.*, **7**, 98–107, 1959.

Japan Meteorological Agency, *Quart, J. Seismology*, **22**, Suppl. Vol., 1957.

Koto, B., On the cause of the great earthquake in central Japan, *J. Coll. Sci., Imp. Univ. Tokyo*, **5**, 295–353, 1893.

Kubo, A., E. Fukuyama, H. Kawai, and K. Nonomura, NIED seismic moment tensor catalogue for regional earthquakes around Japan: quality test and application, *Tectonophys.*, **356**, 23–48, 2002.

Matsuda, T., Surface faults associated with Nobi (Mino-Owari) earthquake of 1891, Japan, *Spec. Rep. Earthq. Res. Inst.*, **13**, 85–126, 1974 (in Japanese).

Mikumo, T. and M. Ando, A search into the faulting mechanism of the 1891 great Nobi earthquake, *J. Phys. Earth*, **24**, 63–87, 1976.

Muramatu, I., Magnitude of the Nobi earthquake of Oct. 28, 1891, *Zisin (J. Seismol. Soc. Jpn.)*, **15**, 341–342, 1962 (in Japanese).

Muramatu, I., Distribution of seismic intensity and crustal deformation in the region destroyed by the great Nobi earthquake of October 28, 1891, *Res. Rep., Gifu Univ.* **3**, 202–224, 1963 (in Japanese).

Nakano, M., J. Miyakoshi, and K. Yamaoka, A new model for the fault beneath sedimentary basin in the 1891 Nobi earthquake, *Earth Planets. Space*, **59**, 13–19, 2007.

Omori, F., Note on the great Mino–Owari earthquake of Oct. 28th, 1891, *Publ. Earthq. Inv. Comm.*, **4**, 13–24, 1900.

Ooida, T., I. Yamada, T. Tada, K. Ito, K. Sugiyama, and Y. Sasaki, Microearthquake activity in central Honshu, Japan, Part I. Seismicity of microearthquakes in the vicinity of the Neo Valley fault, *Zisin (J. Seismol. Soc. Jpn.)*, **24**, 240–247, 1971 (in Japanese).

Saikia, C. K., Modeling of strong ground motions from the 16 September 1978 Tabas, Iran, earthquake, *Bull. Seism. Soc. Am.*, **84**, 31–46, 1994.

Sugisaki, R. and K. Shibata, Reappraisal of the Gifu–Ichinomiya fault—Points at issue for recognition of concealed fault under alluvial plain—, *Zisin (J. Seismol. Soc. Jpn.)*, **56**, 281–296, 2003 (in Japanese).

E. Fukuyama (e-mail: fuku@bosai.go.jp), I. Muramatu, and T. Mikumo